Optically controlled phase gate for two spin qubits in coupled quantum dots

Li-Bo Chen,[1,2] L. J. Sham,[2,*] and Edo Waks[3]

[1]*Department of Physics, Ocean University of China, Qingdao 266100, People's Republic of China*
[2]*Center for Advanced Nanoscience, Department of Physics, University of California-San Diego, La Jolla, California 92093-0319, USA*
[3]*Joint Quantum Institute, University of Maryland and National Institute of Standards and Technology, College Park, Maryland 20742, USA*

We present a feasible scheme for performing an optically controlled phase gate between two conduction electron spin qubits in adjacent self-assembled quantum dots. Interaction between the dots is mediated by the tunneling of the valence hole state, which is activated only by applying a laser pulse of the right polarization and frequency. Combining the hole tunneling with the Pauli blocking effect, we obtain conditional dynamics for the two quantum dots, which is the essence of our gating operations. Our results are of explicit relevance to the recent generation of vertically stacked self-assembled InAs quantum dots, and show that by a design which avoids unintended dynamics the gate could be implemented in theory in the 10-ps range and with a fidelity over 90%. Our proposal therefore offers an accessible path to the demonstration of ultrafast quantum logic in quantum dots.

I. INTRODUCTION

Self-assembled semiconductor quantum dots (SAQDs) possess many properties similar to real atoms, while simultaneously providing highly tunable properties for controlling and manipulating individual electron spins.[1,2] Such SAQDs are promising candidates as qubits for quantum computation, owing in part to the long coherence time[3–5] and high speed for optical coherent control.[6,7] Recently, much progress has been made using dot spin qubits to satisfy the DiVincenzo criteria for quantum computation,[8] such as spin initialization,[9–11] the coherent manipulation of electron spins,[6,12] and fast spin nondestructive measurement.[13]

A fundamental element in quantum computation is the entangling two-qubit quantum gate. A number of theoretical protocols for two-qubit gate have been proposed, including through optical Rudemann-Kittel-Kasuya-Yoshida interaction,[14] Coulomb or tunneling interactions between excited state in neighboring dots,[15–18] long-range coupling through waveguide-cavity system,[19] and phonon-assisted Zeno effect.[20] These schemes have yet to be demonstrated experimentally, however.

Recently, ultrafast optical entanglement control utilizing the *ground-state* conduction *electron tunneling* between two quantum-dot spins was experimentally realized.[21] In this paper, we investigate an approach that takes advantage of the same type of vertically stacked SAQDs in order to entangle the two conduction electron spins in the dots, using the *excited* valence *hole tunneling* as a means to couple the two electron spins. By adjusting the voltage of the Schottky diode which houses the dots so that the two hole levels line up when one of the two electrons are optically excited into a trion, we avoid the tunnel coupling of the two-electron spin qubits when there is no optical excitation. This method enables simpler single-qubit operations. The key physics to accomplish a controlled phase gate is an optical rotation of only one basis state of the two spins to change its sign, utilizing Pauli blocking to prevent the unwanted transformation of the remaining three basis states. Our computed results indicate that by using three laser pulses a controlled phase gate with a fidelity

exceeding 90% can be implemented on a time scale as short as 10 ps.

II. THE BASIC MODEL

The sample under study contains two vertically coupled SAQDs embedded in a Schottky diode structure (Fig. 1).[22–24] The two vertically stacked self-assembled InAs/GaAs quantum dots (QDs) are separated by a thin GaAs barrier such that the electrons or holes can tunnel between the two dots. The two QDs have different thicknesses so that they have different optical transition energies. As a result they can be optically addressed separately with resonant laser frequencies. The nominal height of dot 1, h_1, is greater than that of dot 2, h_2, so that dot 1 exhibits the lower transition energy. This allows the hole levels to be brought into resonance by adjusting the Schottky diode voltage V, while the electron level of dot 2 is shifted to a higher energy than that of dot 1. This is a preliminary step and not part of the quantum information processing.

Figure 2 shows the electron spin states and the lowest trion levels for each QD.[11,25,26] The qubit states are $|\uparrow\rangle$ and $|\downarrow\rangle$, parallel or antiparallel to the x axis (the growth and optical axis). The interband transition is to the trion state, consisting of two electrons in a singlet state and a heavy hole. The two trion levels are $|\uparrow\downarrow\Uparrow\rangle = \frac{1}{\sqrt{2}}(|\uparrow\downarrow\rangle - |\downarrow\uparrow\rangle)|\Uparrow\rangle$ and $|\uparrow\downarrow\Downarrow\rangle = \frac{1}{\sqrt{2}}(|\uparrow\downarrow\rangle - |\downarrow\uparrow\rangle)|\Downarrow\rangle$, where $|\Uparrow\rangle = |\frac{3}{2}, \frac{3}{2}\rangle$ and $|\Downarrow\rangle = |\frac{3}{2}, -\frac{3}{2}\rangle$ denote heavy hole states with spin $3/2$ and $-3/2$ components along x. Optical selection rules dictate that the σ^+ polarization could couple the transition from $|\uparrow\rangle$ to $|\uparrow\downarrow\Uparrow\rangle$, and the σ^- polarization could couple the transition from $|\downarrow\rangle$ to $|\downarrow\uparrow\Downarrow\rangle$. Here, we have neglected hole mixing and assumed that the in-plane magnetic field is zero, conditions to be relaxed later.

III. IMPLEMENTATION OF A TWO-QUBIT PHASE GATE

Among the entangling two-qubit quantum gates, one which is well suited for realizing with atomlike systems such as QDs is the phase gate. The ideal phase gate aims at a phase change
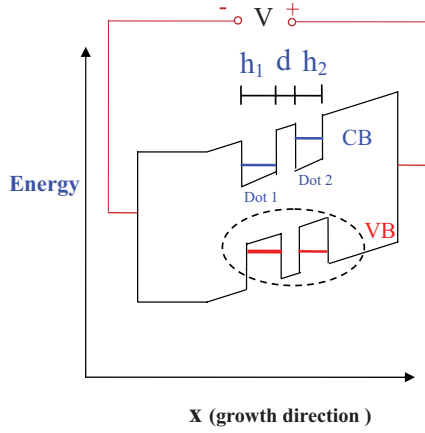
FIG. 1. (Color online) Schematic diagram of the vertically coupled QD system.[22,23] The height of the dot 1 is h_1, that of dot 2 is h_2, and the interdot barrier is d. The hole levels can be brought into resonance by adjusting the Schottky diode voltage V.

in the basis state $|\uparrow\rangle_1|\downarrow\rangle_2$ without affecting the phases of the other three states. It should also preserve the phase coherence of a superposition of the four QD spin states. This operation is a unitary transformation:

$$
\begin{aligned}
|\downarrow\rangle_1|\downarrow\rangle_2 &\rightarrow |\downarrow\rangle_1|\downarrow\rangle_2, \\
|\downarrow\rangle_1|\uparrow\rangle_2 &\rightarrow |\downarrow\rangle_1|\uparrow\rangle_2, \\
|\uparrow\rangle_1|\downarrow\rangle_2 &\rightarrow -|\uparrow\rangle_1|\downarrow\rangle_2, \\
|\uparrow\rangle_1|\uparrow\rangle_2 &\rightarrow |\uparrow\rangle_1|\uparrow\rangle_2.
\end{aligned}
\tag{1}
$$

We use the convention that the vertical arrows in the first and second kets are, respectively, the directions of the spins in dot 1 and dot 2.

To obtain the two-qubit phase gate, we first use a σ^- polarized π pulse to excite the dot 1 spin down state to the trion state. After waiting for a time interval allowing the hole of the trion state to tunnel from dot 1 to dot 2, we apply a σ^- 2π laser pulse to rotate the dot 2 spin-down state via its trion state. The Pauli blocking given by the tunneling hole guarantees that only the $|\uparrow\rangle_1|\downarrow\rangle_2$ state of the two spins undergoes 2π Rabi rotation
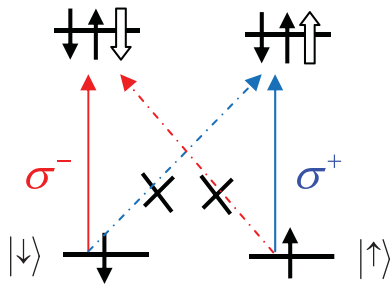

FIG. 2. (Color online) The level diagram of a charged QD with the one-electron spin states and the optically allowed transitions to the trion states. The short solid arrows represent electrons and the short open arrows represent heavy holes. All the arrows are aligned in the x direction. Long arrows with solid lines indicate allowed optical transitions with σ^+ and σ^- denoting two orthogonal circular polarizations. Long arrows with dotted lines and the crosses (X) denote optical transitions are forbidden.
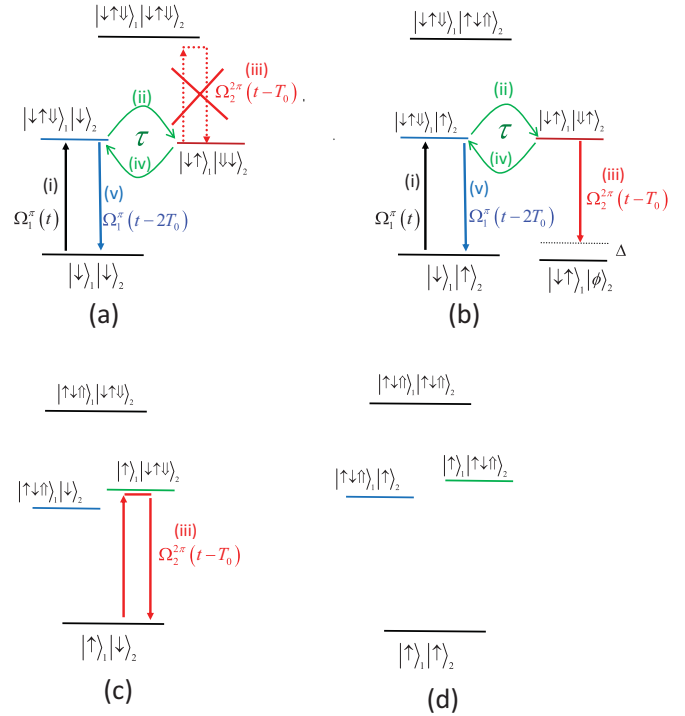

FIG. 3. (Color online) The gate operation process and dynamics of the system under different initial states. The labels (i)–(v) correspond to the operation steps. τ is the hole tunneling between the two dots. (a)–(c) (i) If the electron in QD 1 is spin down, the trion state can be excited by the laser pulse $\Omega_1^\pi(t)$, thus the state $|\downarrow\rangle_1|m\rangle_2$ ($m = \downarrow, \uparrow$) to $|\downarrow\uparrow\Downarrow\rangle_1|m\rangle_2$. (ii) The hole of the trion in QD 1 tunnels to the QD2, thus the state $|\downarrow\uparrow\Downarrow\rangle_1|m\rangle_2$ to $|\downarrow\uparrow\rangle_1|\Downarrow m\rangle_2$. (iii) The laser pulse $\Omega_2^{2\pi}(t - T_0)$ performing a 2π rotation between $|\uparrow\rangle_1|\downarrow\rangle_2$ and $|\uparrow\rangle_1|\downarrow\uparrow\Downarrow\rangle_2$ acquiring the π phase shift, while transition of state $|\downarrow\uparrow\rangle_1|\Downarrow\downarrow\rangle_2$ is forbidden because of Pauli blocking (denoted by the large X). Ideally, the same pulse does not cause the transition between $|\downarrow\uparrow\rangle_1|\Downarrow\uparrow\rangle_2$ and $|\downarrow\uparrow\rangle_1|\phi\rangle_2$ (where ϕ denotes the vacuum state) because excited energy difference between exciton and trion Δ makes this transition to be off resonance. (iv) The state $|\downarrow\uparrow\rangle_1|\Downarrow m\rangle_2$ tunnels back to $|\downarrow\uparrow\Downarrow\rangle_1|m\rangle_2$. (v) The laser pulse $\Omega_1^\pi(t - 2T_0)$ deexcites the trion state in dot 1, thus the state $|\downarrow\uparrow\Downarrow\rangle_1|m\rangle_2$ back to $|\downarrow\rangle_1|m\rangle_2$. (d) If the electrons in both QDs are spin up, they are not affected by the σ^- polarized laser pulses.

and acquires the -1 factor, thus realizing a conditional phase gate. After allowing the hole tunnels back to QD 1, we use another π laser pulse to deexcite the trion state in dot 1. The system will return to its original state with a controlled phase shift. Figure 3 shows the gate operation process and dynamics of the system under different initial states. The detailed gate operation process are as follows.

(i) An ultrafast σ^- polarized π pulse [marked $\Omega_1^\pi(t)$] is applied to excite the dot 1 spin-down state to the trion state, thus, the state $|\downarrow\rangle_1|m\rangle_2$ ($m = \downarrow, \uparrow$) to $-i|\downarrow\uparrow\Downarrow\rangle_1|m\rangle_2$ (for details, see the Appendix).

(ii) We utilize the free evolution of the tunnel process by the Hamiltonian (in the subspace of two tunneling states $[|\downarrow\uparrow\Downarrow\rangle_1|m\rangle_2, |\downarrow\uparrow\rangle_1|\Downarrow m\rangle_2]$)

$$
H_t = \begin{pmatrix} 0 & \tau \\ \tau & 0 \end{pmatrix},
\tag{2}
$$

where τ is the hole-tunneling rate between the two dots. After a precise time $t_1 = T_0 = \pi/(2\tau)$, the state $-i|\downarrow\uparrow\Downarrow\rangle_1|m\rangle_2$ will evolve to $-|\downarrow\uparrow\rangle_1|\Downarrow m\rangle_2$. In the two steps of the process, the states $|\uparrow\rangle_1|\uparrow\rangle_2$ and $|\uparrow\rangle_1|\downarrow\rangle_2$ are not affected by the laser pulse.

(iii) An ultrafast σ^- polarized 2π pulse [marked $\Omega_2^{2\pi}(t - T_0)$] rotates the single trion state in dot 2. The state $|\uparrow\rangle_1|\downarrow\rangle_2$ makes a complete 2π rotation through the state $|\uparrow\rangle_1|\downarrow\uparrow\Downarrow\rangle_2$ and thereby acquires an extra π phase shift,

$$|\uparrow\rangle_1|\downarrow\rangle_2 \rightarrow -|\uparrow\rangle_1|\downarrow\rangle_2. \qquad (3)$$

The transition from the state $|\downarrow\uparrow\rangle_1|\Downarrow\downarrow\rangle_2$ to $|\downarrow\uparrow\rangle_1|\Downarrow\downarrow,\uparrow\Downarrow\rangle_2$ and back is forbidden by the Pauli exclusion principle. Ideally, the same pulse does not cause the transition between $|\downarrow\uparrow\rangle_1|\Downarrow\uparrow\rangle_2$ and $|\downarrow\uparrow\rangle_1|\phi\rangle_2$ (where ϕ denotes the vacuum state) because the excited energy difference between the exciton and trion Δ makes this transition to be off resonance. We consider the possible deviation from the ideal process later.

(iv) We utilize the hole tunneling again. After time $t_2 = T_0 = \pi/(2\tau)$, the state $-|\downarrow\uparrow\rangle_1|\Downarrow m\rangle_2$ tunnels back to $i|\downarrow\uparrow\Downarrow\rangle_1|m\rangle_2$.

(v) Another ultrafast σ^- polarized π pulse [marked as $\Omega_1^\pi(t - 2T_0)$] deexcites the trion state in dot 1 and thus the state $i|\downarrow\uparrow\Downarrow\rangle_1|m\rangle_2$ back to $|\downarrow\rangle_1|m\rangle_2$. The state $|\downarrow\rangle_1|m\rangle_2$ is unchanged by the entire sequence of operations because it is equivalent to two complete state rotations.

Table I summarizes the state evolution, in which the first row numbers the operation steps, the second row shows the time sequence of the pulse, and each subsequent row shows how the evolution of a basis state in the first column transforms in time.

The alternate expression for the phase gate in the basis $[|-z\rangle_1|-z\rangle_2, |-z\rangle_1|+z\rangle_2, |+z\rangle_1|-z\rangle_2, |+z\rangle_1|+z\rangle_2]$ is

$$\frac{1}{2}\begin{bmatrix} 1 & 1 & -1 & 1 \\ 1 & 1 & 1 & -1 \\ -1 & 1 & 1 & 1 \\ 1 & -1 & 1 & 1 \end{bmatrix},$$

and in the basis $[|\downarrow\rangle_1|-z\rangle_2, |\downarrow\rangle_1|+z\rangle_2, |\uparrow\rangle_1|-z\rangle_2, |\uparrow\rangle_1|+z\rangle_2]$ is

$$\begin{bmatrix} 1 & 0 & 0 & 0 \\ 0 & 1 & 0 & 0 \\ 0 & 0 & 0 & 1 \\ 0 & 0 & 1 & 0 \end{bmatrix},$$

where $|\pm z\rangle$ are electron spin states aligned in the z direction. This expression shows a phase gate in combination with single-qubit rotations being equivalent to an entanglement gate or the controlled-NOT gate.

IV. HOLE MIXING AND UNINTENDED DYNAMICS

For error analysis of the gate operation, we now include the effects of hole mixing and unintended dynamics in our analysis. From the Luttinger Hamiltonian,[27,28] the top four states of the valence hole, rather than the "bare" heavy-hole states $|\frac{3}{2}, \pm\frac{3}{2}\rangle$, are mixed by confinement,

$$h_\pm^\dagger|\phi\rangle = \cos\theta_m|\tfrac{3}{2}, \pm\tfrac{3}{2}\rangle - \sin\theta_m e^{\mp i\phi_m}|\tfrac{3}{2}, \mp\tfrac{1}{2}\rangle, \qquad (4)$$

where $|\frac{3}{2}, \mp\frac{1}{2}\rangle$ are light-hole states aligned in the x direction, and θ_m and ϕ_m are mixing angles. With the mixing, the light-matter interaction Hamiltonian for σ^- polarized light with Rabi frequency $\Omega(t)$ becomes

$$H_- = \frac{\Omega(t)}{2}\sum_{i=1,2}(\cos\theta_m e_{i\uparrow}^\dagger h_{i-}^\dagger - \sqrt{1/3}\sin\theta_m e^{-i\phi_m} e_{i\downarrow}^\dagger h_{i+}^\dagger)$$
$$+ \text{H.c.}, \qquad (5)$$

where $i = 1, 2$ denote the two QDs. A σ^+ polarized laser pulse with Rabi frequency $\Omega(t)$ has the Hamiltonian

$$H_+ = \frac{\Omega(t)}{2}\sum_{i=1,2}(\cos\theta_m e_{i\downarrow}^\dagger h_{i+}^\dagger - \sqrt{1/3}\sin\theta_m e^{i\phi_m} e_{i\uparrow}^\dagger h_{i-}^\dagger)$$
$$+ \text{H.c.}, \qquad (6)$$

where the factor of $\sqrt{1/3}$ in the second term comes from the different weights of in-plane components of the valence-band wave functions. However, by adjusting the polarizations of the laser, one may establish the actual axis about which the laser pulse will rotate the state.[29] Instead of σ^- polarized pulse, the new one has the polarization

$$\sigma = (1 - 2/3\sin^2\theta_m)^{-1/2}$$
$$\times (\cos\theta_m\sigma^- + \sqrt{1/3}\sin\theta_m e^{-i\phi_m}\sigma^+), \qquad (7)$$

and Rabi frequency $\Omega(t)$, the Hamiltonian can be written as

$$H_\sigma = \sum_{i=1,2}\frac{\Omega_{\text{eff}}}{2}e_{i\uparrow}^\dagger h_{i-}^\dagger + \text{H.c.}, \qquad (8)$$

with the effective Rabi frequency

$$\Omega_{\text{eff}} = \Omega(t)(1 - 2/3\sin^2\theta_m)^{1/2}. \qquad (9)$$

Thus, θ_m and ϕ_m can be obtained by data fitting after measuring the effective Rabi frequencies of laser pulses with different polarizations. The effect of hole mixing is to slightly decrease the effective Rabi frequency Ω_{eff}, and this can simply be compensated by a proportionate increase in $\Omega(t)$. Use of this new polarization therefore allows us to account for the effects of hole mixing and proceed directly as outlined in the previous sections.

TABLE I. The operation steps, pulse sequence, and state evolution.

Operation step	(i)	(ii)	(iii)	(iv)	(v)
Pulse	$\Omega_1^\pi(t)$	t_1	$\Omega_2^{2\pi}(t - T_0)$	t_2	$\Omega_1^\pi(t - 2T_0)$
$\|\downarrow\rangle_1\|\downarrow\rangle_2$	$-i\|\downarrow\uparrow\Downarrow\rangle_1\|\downarrow\rangle_2$	$-\|\downarrow\uparrow\rangle_1\|\Downarrow\downarrow\rangle_2$	$-\|\downarrow\uparrow\rangle_1\|\Downarrow\downarrow\rangle_2$	$i\|\downarrow\uparrow\Downarrow\rangle_1\|\downarrow\rangle_2$	$\|\downarrow\rangle_1\|\downarrow\rangle_2$
$\|\downarrow\rangle_1\|\uparrow\rangle_2$	$-i\|\downarrow\uparrow\Downarrow\rangle_1\|\uparrow\rangle_2$	$-\|\downarrow\uparrow\rangle_1\|\Downarrow\uparrow\rangle_2$	$-\|\downarrow\uparrow\rangle_1\|\Downarrow\uparrow\rangle_2$	$i\|\downarrow\uparrow\Downarrow\rangle_1\|\uparrow\rangle_2$	$\|\downarrow\rangle_1\|\uparrow\rangle_2$
$\|\uparrow\rangle_1\|\downarrow\rangle_2$	$\|\uparrow\rangle_1\|\downarrow\rangle_2$	$\|\uparrow\rangle_1\|\downarrow\rangle_2$	$-\|\uparrow\rangle_1\|\downarrow\rangle_2$	$-\|\uparrow\rangle_1\|\downarrow\rangle_2$	$-\|\uparrow\rangle_1\|\downarrow\rangle_2$
$\|\uparrow\rangle_1\|\uparrow\rangle_2$	$\|\uparrow\rangle_1\|\uparrow\rangle_2$	$\|\uparrow\rangle_1\|\uparrow\rangle_2$	$\|\uparrow\rangle_1\|\uparrow\rangle_2$	$\|\uparrow\rangle_1\|\uparrow\rangle_2$	$\|\uparrow\rangle_1\|\uparrow\rangle_2$

In order to avoid the unintended excited transition $|\downarrow\uparrow\rangle_1|\Downarrow\uparrow\rangle_2 \rightarrow |\downarrow\uparrow\rangle_1|\phi\rangle_2$ caused by the ultrafast laser pulse $\Omega_2^{2\pi}(t)$, we propose a remedy by pulse shaping.[30] Instead of a 2π single pulse $\Omega_2^{2\pi}(t)$, we use a combination of two phase-locked pulses of σ^- polarization, resonant respectively with the transitions $|\uparrow\rangle_1|\downarrow\rangle_2 \rightarrow |\uparrow\rangle_1|\downarrow\uparrow\Downarrow\rangle_2$ and $|\downarrow\uparrow\rangle_1|\Downarrow\uparrow\rangle_2 \rightarrow |\downarrow\uparrow\rangle_1|\phi\rangle_2$,

$$\begin{aligned}\Omega_2(t) = \Omega_2^0(&\exp[-(t/s)^2 - i\epsilon_2 t]\\&- \exp[-(t/s_1)^2 - i(\epsilon_2 + \Delta)t]),\end{aligned} \quad (10)$$

where ϵ_2 $(\epsilon_2 + \Delta)$ is the trion (exciton) excited energy of QD 2. We choose the parameters satisfying the conditions

$$\begin{aligned}\Omega_2^0(s - s_1 \exp[-(\Delta s_1/2)^2]) = \sqrt{\pi},\\s_1 - s \exp[-(\Delta s/2)^2] = 0,\end{aligned} \quad (11)$$

so that the pulse can produces a 2π rotation for trion resonance $|\uparrow\rangle_1|\downarrow\rangle_2 \rightarrow |\uparrow\rangle_1|\downarrow\uparrow\Downarrow\rangle_2$ and brings the exciton pseudospin to the original state $|\downarrow\uparrow\rangle_1|\Downarrow\uparrow\rangle_2$.

Other sources of error are the spontaneous emission and the laser intensity-dependent dephasing as a function of temperature. The dominant spontaneous emission path is the direct recombination exciton pair $e_\uparrow^+ h_\downarrow^+$ in the states $|\downarrow\uparrow\Downarrow\rangle_1|m\rangle_2$ ($m = \downarrow,\uparrow,|\downarrow\uparrow\rangle_1|\Downarrow\uparrow\rangle_2$, and $|\uparrow\rangle_1|\downarrow\uparrow\Downarrow\rangle_2$. Experiments[31,32] showed laser intensity dependence of the exciton Rabi oscillations. The temperature-independent effect[31] is unimportant for control. We examine the temperature-dependent effect,[32] which gave the additional rate of exciton pure dephasing $\Gamma_2 \approx AT\Omega^2(t)$ due to the exciton-phonon interaction, where A is a constant, T is the temperature, and Ω is the average Rabi frequency of each pulse. We assess the effects through the numerical integration of the master equation for the system in the Lindblad form.[20,33] Experiments have shown that the lifetime of the exciton is of the order of $t_e = 1$ ns.[34,35] We choose the laser pulses, $\Omega_1^\pi(t) = \frac{\sqrt{\pi}}{2s} \exp[-t^2/s^2 - i\epsilon_1 t]$, where ϵ_1 is the trion excited energy of QD 1, $\Omega_2(t)$ is defined by Eqs. (10) and (11), with $s = 0.2$ ps, $\Delta = 4$ meV,[36] and the tunneling $\tau = 2$ meV,[24] $T_0 = \pi/(2\tau) = 3.27$ ps, $T = 1$ K, $A = 11$ fs K^{-1} taken from Ref. 32. For the initial state

$$|\Psi^0\rangle = \tfrac{1}{2}(|\downarrow\rangle_1|\downarrow\rangle_2 + |\downarrow\rangle_1|\uparrow\rangle_2 + |\uparrow\rangle_1|\downarrow\rangle_2 + |\uparrow\rangle_1|\uparrow\rangle_2), \quad (12)$$

the dynamics of the density matrix elements $\rho(|\downarrow\rangle_1\langle\downarrow| \otimes |\downarrow\rangle_2\langle\downarrow|)$, $\rho(|\downarrow\rangle_1\langle\downarrow| \otimes |\uparrow\rangle_2\langle\uparrow|)$, $\rho(|\uparrow\rangle_1\langle\uparrow| \otimes |\downarrow\rangle_2\langle\downarrow|)$, and $\rho(|\uparrow\rangle_1\langle\uparrow| \otimes |\downarrow\rangle_2\langle\uparrow|)$ are shown in Fig. 4. The figure shows the key feature of the phase gate that, after the $\Omega_2(t)$ pulse, the joint two-qubit coherence (or off-diagonal element) $\rho(|\uparrow\rangle_1\langle\uparrow| \otimes |\downarrow\rangle_2\langle\uparrow|)$ gains a minus sign. Simultaneously, the joint "up-down" population, $\rho(|\uparrow\rangle_1\langle\uparrow| \otimes |\downarrow\rangle_2\langle\downarrow|)$, returns to its original value after the 2π rotation. Similarly, both the "down-down" and "down-up" populations, $\rho(|\downarrow\rangle_1\langle\downarrow| \otimes |\downarrow\rangle_2\langle\downarrow|)$, $\rho(|\downarrow\rangle_1\langle\downarrow| \otimes |\uparrow\rangle_2\langle\uparrow|)$, return to their initial values with visible errors after the pulses $\Omega_1^\pi(t)$ and $\Omega_1^\pi(t - 2T_0)$. The "up-up" populations, $\rho(|\uparrow\rangle_1\langle\uparrow| \otimes |\uparrow\rangle_2\langle\uparrow|)$, not shown in the figure, are unchanged by the gate operation. The figure also shows that the total time of implementing the phase gate is $T_g \approx 7$ ps. We calculate the fidelity of the phase gate $F = 0.956$. Besides the spontaneous emission, the error of
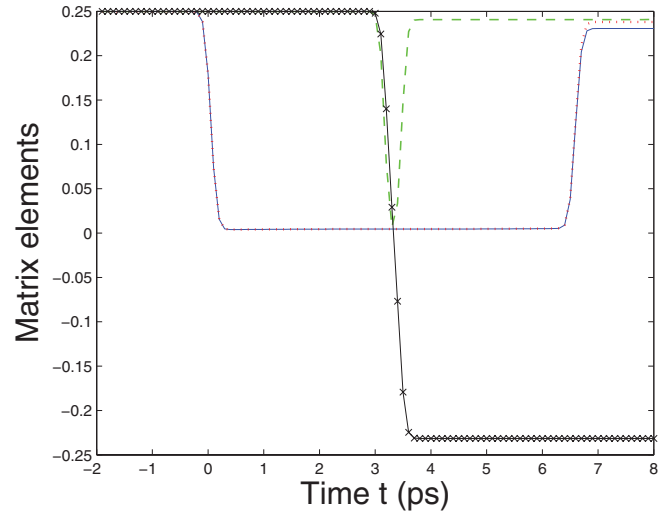

FIG. 4. (Color online) Dynamical evolution of selected density matrix elements for the initial state $|\Psi^0\rangle$ in Eqs. (10) during the gate operation via numerical simulation. The selected density matrix elements are $\rho(|\downarrow\rangle_1\langle\downarrow| \otimes |\downarrow\rangle_2\langle\downarrow|)$ denoted by the solid (blue) line, $\rho(|\downarrow\rangle_1\langle\downarrow| \otimes |\uparrow\rangle_2\langle\uparrow|)$ the dotted (red) line, $\rho(|\uparrow\rangle_1\langle\uparrow| \otimes |\downarrow\rangle_2\langle\downarrow|)$ the dashed (green) line, and $\rho(|\uparrow\rangle_1\langle\uparrow| \otimes |\downarrow\rangle_2\langle\uparrow|)$ the ×-marked (black) line.

tunneling time also decreases the fidelity of the gate. For a 10% error in the tunneling time, the fidelity is further reduced to $F = 0.94$.

Figure 5 shows the notable effect of the temperature and intensity-dependent exciton dephasing on the fidelity of the phase gate as a function of the pulse duration s and for the temperatures $T = 0$–4 K, with the parameters in the caption.
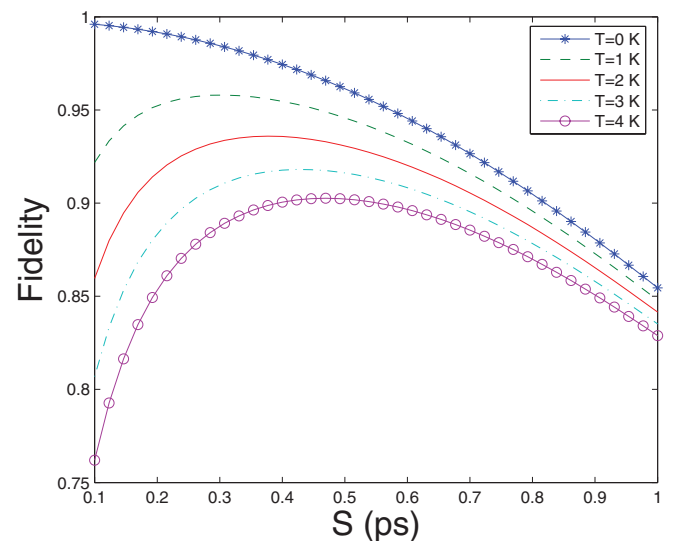

FIG. 5. (Color online) Fidelity of the phase gate as a function of the pulse duration S and for the temperatures $T = 0$–4 K, with the parameters $\Delta = 4$ meV, $g_z^e = 0.48$, $g_z^h = 0.31$, $\tau = 2$ meV, $t_e = 1$ ns, and $A = 11$ fs K^{-1} (Ref. 32).

V. COMPATIBILITY WITH SINGLE-QUBIT ROTATION

In addition to a two-qubit phase gate, single-qubit rotations are required to demonstrate universal quantum computing. In order to make our operation compatible with the single qubit rotation schemes in Refs. 29 and 37, a static magnetic field B is required in the z direction (perpendicular to the growth direction x). The single-qubit operations can be performed by using off-resonance Raman processes through the virtual excitation of an exciton of a single dot. The QDs can be optically addressed separately with resonant laser frequencies.

The application of the magnetic field renders the qubits in the phase gate no longer energy eigenstates. Consequently, the effect of the magnetic field on the fidelity of the gate has to be examined. The qubit states, $|\uparrow\rangle = \frac{1}{\sqrt{2}}(|+z\rangle + |-z\rangle)$ and $|\downarrow\rangle = \frac{1}{\sqrt{2}}(|+z\rangle - |-z\rangle)$, now precess about the z axis at the Larmor frequency $g_z^e \mu_B B/\hbar$, where g_z^e is the effective electron in-plane g factor and μ_B is the Bohr magneton. The excited hole states are $|\Uparrow\rangle$ and $|\Downarrow\rangle$ and precess at the frequency $g_z^h \mu_B B/\hbar$, where g_z^h is the effective hole in-plane g factor. To find the magnetic-field effect on the phase gate fidelity, we calculate the dynamics of the system using the measured values[11] $g_z^e = 0.48$, $g_z^h = 0.31$ and the Gaussian pulses, $\Omega_1^\pi(t) = \frac{\sqrt{\pi}}{2s}\exp[-t^2/s^2 - i\epsilon_1 t]$, with $\Omega_2(t)$ defined by Eqs. (10) and (11), $\Delta = 4$ meV, the tunneling $\tau = 2$ meV, $T_0 = \pi/(2\tau) = 3.27$ ps, the trion lifetime $t_e = 1$ ns, $A = 11$ fs K^{-1}, and the temperature $T = 1$ K. For an initial state $|\Psi^0\rangle$ in Eq. (12), we plot the phase gate fidelity F as a function of the magnetic field B and the inverse pulse duration s^{-1} in Fig. 6. We can see that the fidelity decreases with increasing magnetic field, because the bandwidth of the gate pulses must be larger than the Zeeman splitting. The controlled phase gate

can be implemented with a fidelity over 0.90 in the case of $B = 1$ T and $s^{-1} = 1$ THz.

VI. CONCLUSION

In conclusion, we have proposed a controlled-phase gate for two coupled SAQDs in the Voigt configuration, which is compatible with the previously designed single-qubit rotations.[29,37] The speed of our gate is essentially limited by the hole tunneling between the two QDs. In Ref. 21 the tunneling of the electron is always coupling the two spins of QDs, which enables simpler two-qubit rotation while more difficult single-qubit operations than our scheme. We have shown that hole mixing can be simply incorporated into this scheme through a change in laser polarization. The result shows that we could implement the gate in the 10-ps range and fidelity over 90%. Our proposal therefore offers an accessible path to the demonstration of ultrafast quantum logic in SAQDs.

APPENDIX: EXCITATION OF THE DOT 1 SPIN-DOWN STATE TO THE TRION STATE

The coupled SAQDs are illuminated with a σ^- circularly polarized laser pulse propagating in the x direction. The laser is tuned such that it could create an exciton in the QD 1, only if its state is $|\downarrow\rangle$. This will not affect the QD 2 because a trion in the smaller dot 2 is tens of millielectron volts (meVs) higher than dot 1 in energy.[21] In the subspaces $[|\downarrow\rangle_1|m\rangle_2, |\downarrow\uparrow\downarrow\rangle_1|m\rangle_2, |\downarrow\uparrow\rangle_1|\downarrow m\rangle_2]$ ($m = \downarrow$, $\uparrow$), the Hamiltonian for the QDM under this laser excitation is

$$H = \begin{pmatrix} 0 & \frac{\Omega_0}{2} & 0 \\ \frac{\Omega_0}{2} & 0 & \tau \\ 0 & \tau & 0 \end{pmatrix}, \qquad (A1)$$

where the energy is in units of $\hbar$, Ω_0 is the Rabi frequency of the laser pulse, and τ is the hole tunneling rate between the two dots. Transforming the basis set of the excited hole states, one in each dot, to a basis of tunneling eigenstates, $|\Phi^\pm\rangle = 2^{-1/2}(|\downarrow\uparrow\downarrow\rangle_1|m\rangle_2 \pm |\downarrow\uparrow\rangle_1|\downarrow m\rangle_2)$, we have

$$H = \begin{pmatrix} 0 & \frac{\Omega_0}{2\sqrt{2}} & \frac{\Omega_0}{2\sqrt{2}} \\ \frac{\Omega_0}{2\sqrt{2}} & -\tau & 0 \\ \frac{\Omega_0}{2\sqrt{2}} & 0 & \tau \end{pmatrix}. \qquad (A2)$$
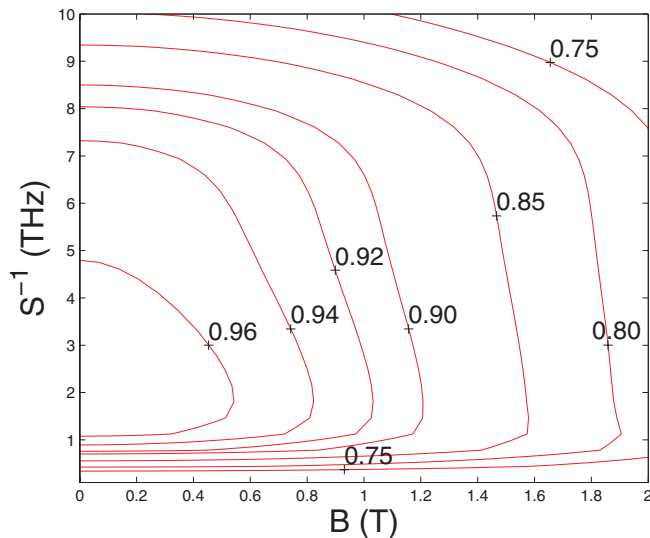

FIG. 6. (Color online) Contour plot of the phase gate fidelity F for the initial state $|\Psi^0\rangle$ in Eqs. (12) as a function of the magnetic field B and the inverse pulse duration s^{-1} with the parameters $\Delta = 4$ meV, $g_z^e = 0.48$, $g_z^h = 0.31$, $\tau = 2$ meV, $t_e = 1$ ns, $T = 1$ K, and[32] $A = 11$ fs K^{-1}.

Starting with the initial state $|\downarrow\rangle_1|m\rangle_2$, the system evolves at the time t to

$$|\psi(t)\rangle = \frac{1}{\sqrt{2}(\tau^2 + \Omega_0^2/4)} \begin{pmatrix} \sqrt{2}\tau^2 + \sqrt{2}\Omega_0^2/4 \cos\left(t\sqrt{\tau^2 + \Omega_0^2/4}\right) \\ -i\Omega_0/2\sqrt{\tau^2 + \Omega_0^2/4}\sin\left(t\sqrt{\tau^2 + \Omega_0^2/4}\right) + \tau\Omega_0/2\cos\left(t\sqrt{\tau^2 + \Omega_0^2/4}\right) - \tau\Omega_0/2 \\ -i\Omega_0/2\sqrt{\tau^2 + \Omega_0^2/4}\sin\left(t\sqrt{\tau^2 + \Omega_0^2/4}\right) - \tau\Omega_0/2\cos\left(t\sqrt{\tau^2 + \Omega_0^2/4}\right) + \tau\Omega_0/2 \end{pmatrix}. \quad (A3)$$

At time $t_0 = \pi/(2\sqrt{\tau^2 + \Omega_0^2/4})$, the state is

$$|\psi(t_1)\rangle = \frac{1}{\sqrt{2}(\tau^2 + \Omega_0^2/4)} \begin{pmatrix} \sqrt{2}\tau^2 \\ -i\Omega_0/2\sqrt{\tau^2 + \Omega_0^2/4} - \tau\Omega_0/2 \\ -i\Omega_0/2\sqrt{\tau^2 + \Omega_0^2/4} + \tau\Omega_0/2 \end{pmatrix}. \quad (A4)$$

In the case $\Omega_0 \gg \tau$, $t_0 \approx \pi/\Omega_0$, $|\psi(t_1)\rangle \approx \frac{-i}{\sqrt{2}}(|\Phi^+\rangle + |\Phi^-\rangle) = -i|\downarrow\uparrow\Downarrow\rangle_1|m\rangle_2$. So for a sufficiently short-duration π pulse, the equal combination state of the two tunneling eigenstates, $|\Phi^+\rangle$ and $|\Phi^-\rangle$, is created, which corresponds to a localized trion state $|\downarrow\uparrow\Downarrow\rangle_1|m\rangle_2$.

---

*lsham@ucsd.edu

[1] P. M. Petroff, A. Lorke, and A. Imamoglu, Phys. Today **54**(5), 46 (2001).

[2] M. Bayer and A. Forchel, Phys. Rev. B **65**, 041308 (2002).

[3] D. Birkedal, K. Leosson, and J. M. Hvam, Phys. Rev. Lett. **87**, 227401 (2001).

[4] P. Borri, W. Langbein, S. Schneider, U. Woggon, R. L. Sellin, D. Ouyang, and D. Bimberg, Phys. Rev. Lett. **87**, 157401 (2001).

[5] X. Xu, W. Yao, B. Sun, D. G. Steel, A. S. Bracker, D. Gammon, and L. J. Sham, Nature (London) **459**, 1105 (2009).

[6] D. Press, T. D. Ladd, B. Zhang, and Y. Yamamoto, Nature (London) **456**, 218 (2008).

[7] E. D. Kim, K. Truex, X. Xu, B. Sun, D. G. Steel, A. S. Bracker, D. Gammon, and L. J. Sham, Phys. Rev. Lett. **104**, 167401 (2010).

[8] D. P. DiVincenzo, Fortschr. Phys. **48**, 771 (2000).

[9] M. Atature, J. Dreiser, A. Badolato, A. Hogele, K. Karrai, and A. Imamoglu, Science **312**, 551 (2006).

[10] C. Emary, X. Xu, D. G. Steel, S. Saikin, and L. J. Sham, Phys. Rev. Lett. **98**, 047401 (2007).

[11] X. Xu, Y. Wu, B. Sun, Q. Huang, J. Cheng, D. G. Steel, A. S. Bracker, D. Gammon, C. Emary, and L. J. Sham, Phys. Rev. Lett. **99**, 097401 (2007).

[12] E. D. Kim, K. Truex, X. Xu, B. Sun, D. G. Steel, A. S. Bracker, D. Gammon, and L. J. Sham, Phys. Rev. Lett. **104**, 167401 (2010).

[13] D. Kim, S. E. Economou, S. C. Badescu, M. Scheibner, A. S. Bracker, M. Bashkansky, T. L. Reinecke, and D. Gammon, Phys. Rev. Lett. **101**, 236804 (2008).

[14] C. Piermarocchi, P. Chen, L. J. Sham, and D. G. Steel, Phys. Rev. Lett. **89**, 167402 (2002).

[15] T. Calarco, A. Datta, P. Fedichev, E. Pazy, and P. Zoller, Phys. Rev. A **68**, 012310 (2003).

[16] A. Nazir, B. W. Lovett, S. D. Barrett, T. P. Spiller, and G. A. D. Briggs, Phys. Rev. Lett. **93**, 150502 (2004).

[17] E. M. Gauger, A. Nazir, S. C. Benjamin, T. M. Stace, and B. W. Lovett, New J. Phys. **10**, 073016 (2008).

[18] C. Emary and L. J. Sham, Phys. Rev. B **75**, 125317 (2007).

[19] S. M. Clark, Kai-Mei C. Fu, T. D. Ladd, and Y. Yamamoto, Phys. Rev. Lett. **99**, 040501 (2007).

[20] K. J. Xu, Y. P. Huang, M. G. Moore, and C. Piermarocchi, Phys. Rev. Lett. **103**, 037401 (2009).

[21] D. Kim, S. Carter, A. Greilich, A. Bracker, and D. Gammon, Nat. Phys. **7**, 223 (2011).

[22] M. Scheibner, M. F. Doty, I. V. Ponomarev, A. S. Bracker, E. A. Stinaff, V. L. Korenev, T. L. Reinecke, and D. Gammon, Phys. Rev. B **75**, 245318 (2007).

[23] M. F. Doty, J. I. Climente, A. Greilich, M. Yakes, A. S. Bracker, and D. Gammon, Phys. Rev. B **81**, 035308 (2010).

[24] M. F. Doty, J. I. Climente, M. Korkusinski, M. Scheibner, A. S. Bracker, P. Hawrylak, and D. Gammon, Phys. Rev. Lett. **102**, 047401 (2009).

[25] Y. Wu, E. D. Kim, X. Xu, J. Cheng, D. G. Steel, A. S. Bracker, D. Gammon, S. E. Economou, and L. J. Sham, Phys. Rev. Lett. **99**, 097402 (2007).

[26] J. Berezovsky, M. H. Mikkelsen, N. G. Stoltz, L. A. Coldren, and D. D. Awschalom, Science **320**, 349 (2008).

[27] J. M. Luttinger, Phys. Rev. **102**, 1030 (1956).

[28] D. A. Broido and L. J. Sham, Phys. Rev. B **31**, 888 (1985).

[29] C. Emary and L. J. Sham, J. Phys.: Condens. Matter **19**, 056203 (2007).

[30] Pochung Chen, C. Piermarocchi, and L. J. Sham, Phys. Rev. Lett. **87**, 067401 (2001).

[31] T. H. Stievater, X. Li, D. G. Steel, D. Gammon, D. S. Katzer, D. Park, C. Piermarocchi, and L. J. Sham, Phys. Rev. Lett. **87**, 133603 (2001).

[32] A. J. Ramsay, A. M. Fox, M. S. Skolnick, A. V. Gopal, E. M. Gauger, B. W. Lovett, and A. Nazir, Phys. Rev. Lett. **104**, 017402 (2010).

[33] G. Lindblad, Commun. Math. Phys. **48**, 119 (1976).

[34] S. Cortez, O. Krebs, S. Laurent, M. Senes, X. Marie, P. Voisin, R. Ferreira, G. Bastard, J.-M. Gerard, and T. Amand, Phys. Rev. Lett. **89**, 207401 (2002).

[35] C. Bardot, M. Schwab, M. Bayer, S. Fafard, Z. Wasilewski, and P. Hawrylak, Phys. Rev. B **72**, 035314 (2005).

[36] E. A. Stinaff, M. Scheibner, A. S. Bracker, I. V. Ponomarev, V. L. Korenev, M. E. Ware, M. F. Doty, T. L. Reinecke, and D. Gammon, Science **311**, 636 (2006).

[37] Pochung Chen, C. Piermarocchi, L. J. Sham, D. Gammon, and D. G. Steel, Phys. Rev. B **69**, 075320 (2004).